Autocrine 17-β-estradiol/estrogen receptor-α loop determines the response to immune-checkpoint inhibitors in non-small cell lung cancer

This is a postprint version of the article published in *Clinical Cancer Research*

The final published article is available online at https:doi.org https://doi.org/10.1158/1078-0432.CCR-22-3949

Cite this article as Dario P Anobile, Iris C Salaroglio, Fabrizio Tabbò, Sofia La Vecchia, Muhlis Akman, Francesca Napoli, Maristella Bungaro, Federica Benso, Elisabetta Aldieri, Paolo Bironzo, Joanna Kopecka, Francesco Passiglia, Luisella Righi, Silvia Novello, Giorgio V Scagliotti, Chiara Riganti; Autocrine 17-β-Estradiol/Estrogen Receptor-α Loop Determines the Response to Immune Checkpoint Inhibitors in Non-Small Cell Lung Cancer. Clin Cancer Res 2023, 29 (19): 3958–3973

Autocrine 17-β-Estradiol/Estrogen Receptor-α Loop Determines the Response to Immune Checkpoint Inhibitors in Non-Small Cell Lung Cancer

Dario P Anobile[1,#], Iris C Salaroglio[1,#], Fabrizio Tabbò[2,#], Sofia La Vecchia[1], Muhlis Akman[1], Francesca Napoli[3], Maristella Bungaro[2], Federica Benso[3], Elisabetta Aldieri[1], Paolo Bironzo[2], Joanna Kopecka[1], Francesco Passiglia[2], Luisella Righi[3], Silvia Novello[2,#], Giorgio V Scagliotti[2,#], Chiara Riganti[1,4,#]

Affiliations

1 Department of Oncology, University of Torino, Torino, Italy.

2 Thoracic Oncology Unit, Department of Oncology at San Luigi Gonzaga Hospital, University of Torino, Torino, Italy.

3 Pathology Unit, Department of Oncology at San Luigi Gonzaga Hospital, University of Torino, Torino, Italy.

4 Molecular Biotechnology Center "Guido Tarone", University of Torino, Torino, Italy.

# Contributed equally.

Abstract

Purpose:

The response to immune checkpoint inhibitors (ICI) often differs between genders in non–small cell lung cancer (NSCLC), but metanalyses results are controversial, and no clear mechanisms are defined. We aim at clarifying the molecular circuitries explaining the differential gender-related response to anti–PD-1/anti–PD-L1 agents in NSCLC.

Experimental Design:

We prospectively analyzed a cohort of patients with NSCLC treated with ICI as a first-line approach, and we identified the molecular mechanisms determining the differential efficacy of ICI in 29 NSCLC cell lines of both genders, recapitulating patients' phenotype. We validated new immunotherapy strategies in mice bearing NSCLC patient-derived xenografts and human reconstituted immune system ("immune-PDXs").

Results:

In patients, we found that estrogen receptor α (ERα) was a predictive factor of response to pembrolizumab, stronger than gender and PD-L1 levels, and was directly correlated with PD-L1 expression, particularly in female patients. ERα transcriptionally upregulated CD274/PD-L1 gene, more in females than in males. This axis was activated by 17-β-estradiol, autocrinely produced by intratumor aromatase, and by the EGFR-downstream effectors Akt and ERK1/2 that activated ERα. The efficacy of pembrolizumab in immune-PDXs was significantly improved by the aromatase inhibitor letrozole, which reduced PD-L1 and increased the percentage of antitumor CD8+T-lymphocytes, NK cells, and Vγ9Vδ2 T-lymphocytes, producing durable control and even tumor regression after continuous administration, with maximal benefit in 17-β-estradiol/ERα highfemale immune-xenografts.

Conclusions:

Our work unveils that 17-β-estradiol/ERα status predicts the response to pembrolizumab in patients with NSCLC. Second, we propose aromatase inhibitors as new gender-tailored immune-adjuvants in NSCLC.

Introduction

The implementation of immune checkpoint inhibitors (ICI), mainly anti-programmed death 1 (PD-1)/PD-ligand 1 (PD-L1) agents, in the treatment of non–small cell lung cancer (NSCLC), which represents up to 90% of all lung cancers, has significantly improved disease control, although in a limited proportion of patients (≈20%–35%; ref. 1). The levels of PD-L1 and differences in sex, histology, and concurrent treatments are among the main determinants of immunotherapy (IOT) efficacy in NSCLC (1, 2). The role of sex in response to IOT remains controversial and is cancer dependent: melanoma and NSCLC are the tumors most extensively studied in relation to gender, with different results depending on stage and experimental design. Indeed, network metanalyses often reported contrasting results, indicating higher benefits of IOT in males (2–5), in females (6, 7) or no differences between genders (1, 8, 9). Beyond sex-related differences in the mutation burden (9, 10), drug-metabolizing genes (11, 12) and immune-environment (10), the treatment regimen is an additional factor to be considered: indeed, in the same meta-analysis reporting no gender-related benefit of IOT or chemotherapy (1), females had significantly higher benefit from the combination of ICI with chemotherapy than males (1).

Moreover, sexual hormones are critical in cancer progression and treatment, both in hormone-dependent and independent cancers (13). Interestingly, the expression of estrogen receptor (ER) α and β, progesterone receptor (PR), androgen receptor (AR), and aromatase (14, 15), together with the activation of epidermal growth factor receptor (EGFR; ref. 16), concur with the prognosis (17–19). Estrogens stimulate NSCLC tumor progression, either by activating ERα-driven transcriptional programs or synergizing with prosurvival signaling downstream EGFR (20, 21), with higher effects in female than in male xenografts (22). Estrogen protumor activity offers new therapeutic opportunities. For instance, the ERα/β inhibitors tamoxifen (22) and fulvestrant (20) reduce NSCLC growth with higher benefits in female xenografts and can reverse the resistance to cisplatin (23) and to the EGFR inhibitors gefitinib (24) and vandetanib (25). Interestingly, in melanoma 2-metoxyestradiol, the main catabolite of 17-β-estradiol, increases the antitumor activity of CD8+T lymphocytes and enhances the effects of anti–PD-L1 antibody (26). In breast cancer, anti-estrogen drugs also target the ERα present in immune-infiltrating cells, decreasing the immunosuppression induced by myeloid-derived suppressor cells and T-regulatory cells, increasing the M1-polarization of macrophages, the activity of dendritic cells and CD4+/CD8+ T cells, and the efficacy of anti–PD-L1 antibody in mice xenografts (27). A similar positive immune-imprinting exerted by ERα inhibitors has

been reported in other cancers, not considered estrogen-dependent (28). To date, no studies have investigated whether estrogens and ERα/β activity affect the efficacy of anti–PD-1/PD-L1 agents in NSCLC. The aim of this work is to clarify whether and how estrogen-dependent molecular circuitries could explain the differential gender response to IOT observed in clinical studies in NSCLC.

Materials and Methods

Chemicals and materials

Fetal bovine serum (FBS, #A38401) and RPMI1640 culture medium (#61870010) were from Invitrogen Life Technologies. Plasticware for cell culture was from Falcon (Becton Dickinson). Electrophoretic reagents were from Bio-Rad Laboratories. If not otherwise specified, reagents were purchased from Sigma-Aldrich.

Patients' enrollment and follow-up, PD-L1/ERα immunohistochemical analysis

Thirty-five patients (15 females, 20 males; age: 40–79) with advanced NSCLC, PD-L1 tumor proportion score (TPS) ≥50%, and receiving ≥1 dose of pembrolizumab as monotherapy in first-line treatment were prospectively enrolled from 2018 to 2020 and followed up until May 31, 2022, after obtaining written informed consent. Inclusion criteria are: pathologic diagnosis of stage III–IV NSCLC; TPS ≥ 50%; immunotherapy as first-line treatment. Exclusion criteria are: any other pharmacologic or radiotherapy treatment prior or after immunotherapy. Treatment was terminated due to disease progression or unacceptable toxicity. CT scan evaluation was performed at week 12 and every 12 weeks thereafter until disease progression. Responses (partial response, PR; stable disease, SD; progressive disease, PD) were evaluated using the Response Evaluation Criteria in Solid Tumours (RECIST) v1.1. after three cycles and then every two months. Immunohistochemical evaluations of tumor PD-L1 and ERα were performed with anti–PD-L1 (clone 22C3, pharmDx Kit, #SK006; Dako, Agilent Technologies), anti-ERα (#ab75635, Abcam, 1/100; RRID:AB_1310196), antibodies, using the Dako Omnis platform (Agilent Technologies; RRID:SCR_019495). The patients' clinical data compared with NSCLC patients and PD-L1 expression levels as TPS are reported in Supplementary Tables S1 and S2. ERα was quantified as Histoscore (Hscor; ref. 29). The study was conducted in accordance with the Declaration of Helsinki and was approved by the local ethics committee (San Luigi Gonzaga Hospital, Orbassano, Torino; IRB n. 73/2018).

TCGA dataset analysis

Lung adenocarcinoma (LUAD) dataset of The Cancer Genome Atlas (TCGA; RRID:SCR_003193; n = 531 patients; 246 males, 287 females) was imported into R environment. Count matrices and clinical data (gender, overall survival: OS) were extracted and used to create dds object, using DESeq2 package (RRID:SCR_015687). According to the variance stabilizing transformation of dds object, optimal cut points for "high" and "low" levels of ESR1, encoding for ERα, and CD274, encoding for PD-L1, were estimated using surv_cutpoint() function of survminer package (RRID:SCR_021094). The correlation between ESR1high/low or CD274high/low and OS was calculated by the Kaplan–Meier method and log-rank test.

Cell lines

Human NSCLC cell lines (Supplementary Table S3) and breast cancer MCF-7 cell line (#HTB-22; ATCC) were maintained in the respective culture media with 10% v/v FBS and 1% v/v penicillin–streptomycin (#P4333,

Sigma-Aldrich). All cell lines were authenticated by microsatellite analysis using a PowerPlex Kit (#DC2402, Promega Corporation; last authentication: September 2022). Mycoplasma spp. contamination was checked every 3 weeks using RT-PCR, and the contaminated cells were discharged. Cells were used until passage 12 and maintained in culture <3 months.

Flow cytometry

Cells (1 × 104) were washed in PBS, fixed with 4% v/v paraformaldehyde (#158127, Sigma-Aldrich) for 5 minutes, incubated with anti-CD274/PD-L1, fluorescein isothiocyanate (FITC)-conjugated antibody (clone MIH1, #558065; BD Pharmingen; RRID:AB_647176), and washed three times with PBS-FBS 1%. The results were analyzed with a Guava easyCyte flow cytometer (Millipore) using InCyte software (Millipore).

RT-PCR

Total RNA was extracted and reverse-transcribed using an iScript cDNA Synthesis Kit (#1708890, Bio-Rad Laboratories). RT-PCR was performed using the IQ SYBR Green SuperMix (#1708882, Bio-Rad Laboratories). Primer sequences are listed in Supplementary Table S4. Relative quantitation was performed by comparing each PCR product with the housekeeping gene S14, using Bio-Rad Software Gene Expression Quantitation (Bio-Rad Laboratories). PCR arrays were carried out on 1 µg cDNA from tumor extracts, using the Immune Response Tier 1 RT2 Profiler PCR Array and the IFN gamma signaling pathway RT2 Profiler PCR Array (Bio-Rad Laboratories) as per the manufacturer's instructions. Data analysis was performed using the PrimePCR Analysis Software (Bio-Rad Laboratories).

17-β-Estradiol, progesterone, and testosterone measurement

17-β-estradiol, progesterone, and testosterone levels were measured using the Human Estradiol E2 ELISA Kit (#ab108640), Human Progesterone ELISA Kit (#ab108670), and Testosterone ELISA Kit (#ab108666; all from Abcam).

Immunoblot

Cells were lysed in MLB buffer (125 mmol/L Tris-HCl, 750 mmol/L NaCl, 1% v/v NP40, 10% v/v glycerol, 50 mmol/L MgCl2, 5 mmol/L EDTA, 25 mmol/L NaF, 1 mmol/L NaVO4, 10 mg/mL leupeptin, 10 mg/mL pepstatin, 10 mg/mL aprotinin, 1 mmol/L phenylmethylsulfonyl fluoride; pH 7.5), sonicated, and centrifuged at 13,000 × g for 10 minutes at 4°C. Nuclear extracts were prepared with the Nuclear Extract Kit (Active Motif). Thirty micrograms of whole-cell lysate proteins and 10 µg of nuclear proteins were subjected to immunoblotting, using the following antibodies: anti-ERα (#ab75635; Abcam, 1/400; RRID:AB_1310196), anti-phospho(Ser118)ERα (clone E91, #ab32396; Abcam, 1/1000; RRID:AB_732252), anti-PR (clone αPR6, #ab2765; Abcam, 1/500; RRID:AB_2164316), anti-AR [clone ER179 (2), #ab108341; Abcam, 1/2500; RRID:AB_10865716], anti-aromatase (#ab35604; Abcam, 1/800; RRID:AB_867729), anti-EGFR (clone EP38Y, #ab52894; Abcam, 1/5000; RRID:AB_869579), anti-phospho(Thr308)Akt (#05–802R; Millipore, 1/1,000; RRID:AB_1586880), anti-Akt (clone SKB1, #ST1088; Millipore, 1/500; RRID:AB_2224893), anti-phospho(Thr202/Tyr204)-ERK1/2 (#9101, Cell Signaling Technology, 1/1,000; RRID:AB_331646), anti-ERK1/2 (clone 137F5, #4695; Cell Signaling Technology, 1/1,000; RRID:AB_390779), anti–β-tubulin (#sc-5274; Santa Cruz Biotechnology Inc., 1/1,000; RRID:AB_2288090) or anti-TFIID/TATA box-binding protein

(TBP; clone 58C9, #sc-421; Santa Cruz Biotechnology Inc., 1/250; RRID:AB_628344). The proteins were detected by enhanced chemiluminescence (Gel Doc and Image Lab Touch Software, Bio-Rad Laboratories).

Promoter analysis and chromatin immunoprecipitation (ChIP)

Estrogen Response Elements (ERE) on CD274/PD-L1 promoter were identified using the Transfac database (http://genexplain.com/transfac/; RRID:SCR_005620). ChIP samples were prepared as previously described (30) using anti-ERα (clone E115, #ab32063; Abcam, 1/600; RRID:AB_732249) or anti-ERβ (clone 14C8, #GTX70174; Genetex, Irvine, CA, 1/500; RRID:AB_370367) antibodies. Primers for ERE1/ERE2 in CD274/PD-L1 promoter and nonspecific primers mapping 10,000 bp upstream are reported in Supplementary Table S4. The immunoprecipitated products were amplified by RT-PCR. The signal of the non-specific primers was subtracted from the signal of the EREs sequence.

Measurement of Akt, ERK1/2, and EGFR activity and phospho(ser118)ERα

Akt, ERK1/2, and EGFR kinase activities were measured using the TruLight Akt1/PKBα Kinase Assay kit (#539705; Sigma-Aldrich), TruLight ERK1/2 Assay Kit (#539715; Sigma-Aldrich) and EGFR Kinase Assay Kit (#V9261; EGFR Kinase Promega Corporation). Quantification of phospho(Ser118)ERα was performed using the RayBio Human Phospho-Estrogen Receptor (Ser118) ELISA Kit (#PEL-ERa-S118-T-1; RayBiotech).

ER-α overexpression and silencing

NCI-H1385 cells (1 × 106) were transfected with 1 µg of Lenti ORF clone of Human estrogen receptor 1 (ESR1), transcript variant 1, mutant green fluorescent protein (mGFP)-tagged (#RC213277L4; Origene); 1 × 106 NCI-H1975 cells were transduced with 1 µg of lentiviral GFP-plasmid containing 4 unique 29mer shRNA constructs for ESR1 (#TL320346; Origene), using TurboFectin 8.0 (#TF81001; OriGene) as per the manufacturer's instructions.

EGFR knock-out and overexpression

Cells (5 × 105) were transduced with 1 µg CRISPR pCas vector targeting EGFR (EGFR Human Gene Knockout Kit, #KN414877; Origene). Stably knocked-out (KO) cells were selected using 1 µg/mL puromycin for 4 weeks. KO cells (5 × 105) were then transduced with 1 µg EGFR (NM_005228) Human Mutant ORF Clone (L858R; #RC400290; Origene) and selected with 1 mg/mL neomycin for 3 weeks to generate stable clones. The presence of L858R EGFR was verified by RT-PCR using primers provided by the manufacturer.

In vivo experiments

Female-derived NCI-H1385 and NCI-H1975 cells (1 × 106), male-derived A549 and NCI-H1650 cells, and cells derived from female patients #10 and #3 and male patients #25 and #32 (Supplementary Table S2), mixed with 100 µL Matrigel, were injected subcutaneously into NOD.Cg-Prkdcscid Il2rgtm1Wjl (NSG, #005557; The Jackson Laboratory) female mice engrafted with human hematopoietic CD34+cells derived from the same donor, with comparable levels of circulating monocyte- and lymphocyte-derived lineages at baseline (Hu-CD34+NSG; The Jackson Laboratory). Animals were housed (5 per cage) under a 12-hour light/dark cycle, with food and drinking provided ad libitum. Tumor growth was measured daily using a caliper according to the equation (L × W2)/2, where L is the tumor length and W is the tumor width. When the volume reached

100 mm3, mice were randomized. In the first experimental set, animals were treated for 5 weeks with: (i) vehicle: 100 µL saline solution intraperitoneally, once/week; (ii) letrozole (#L6545, Sigma-Aldrich): 1 mg/kg per os daily; (iii) pembrolizumab (#HDBS0006; BioMol): 10 mg/kg i.p. (day 1), then 5 mg/kg i.p. once/week; (iv) pembrolizumab + letrozole. When indicated, 3 additional groups were added: (v) cisplatin (#P4394, Sigma-Aldrich): 2 mg/kg intravenously once/week; (vi) cisplatin + pembrolizumab; (vii) cisplatin + pembrolizumab + letrozole. In the second set, animals were left untreated after day 35 to monitor progression free survival (PFS) and OS. In the third set, animals were treated for 5 weeks with pembrolizumab + letrozole, then divided into three cohorts: the first cohort was left untreated until week 15; the second cohort was treated with 1 mg/kg letrozole until week 15; the third cohort was treated with 1 mg/kg letrozole from week 6 to week 10, followed by pembrolizumab + letrozole from week 11 to week 15. All mice were euthanized with zolazepam (0.2 mL/kg) and xylazine (16 mg/kg). Animals were subjected to euthanasia in the following conditions: tumor growth exceeding 2.0 g (about 2,000 mm3) or 10% of the body mass; body mass reduction by ≥20%; any of these signs: ulceration, paralysis, labored breathe, ascites, diarrhea over 48 hours, failure to eat and drink for more than 24 hours, cyanosis, hypothermia. The animal care and experimental procedures were approved by the Bio-Ethical Committee of the Italian Ministry of Health (#627/2018-PR, 10/08/2018). The researchers analyzing the results were unaware of the treatments.

Tumor cells and tumor-infiltrating lymphocyte analysis

Tumors were resected and digested to obtain single-cell suspensions (31). Tumor cells were isolated using the Tumor Cell Isolation Kit (#130–108–339; Miltenyi Biotec) and stained with anti-CD274/PD-L1 antibody (clone MIH1, #558065; BD Pharmingen). Tumor-infiltrating lymphocyte (TIL), isolated with the Pan T Cell Isolation Kit (#130–096–535, Miltenyi Biotec), were stained with the following antibodies: anti-CD8 (clone BW135/80, #130–113–158, Miltenyi Biotec, 1/10) for CD8+T-lymphocytes, anti-CD56 (clone AF127H3, #130–113–307, Miltenyi Biotec, 1/10) for natural killer (NK) cells, anti-TCR Vγ9 (#555733; BD Pharmingen, 1/10) for Vγ9Vδ2 T-lymphocytes. Each population was co-stained with anti-Ki67 (REA183, #130–117–691, Miltenyi Biotec, 1/10) and anti-INFγ (REA600, #130–113–495, Miltenyi Biotec, 1/10) antibodies. Cells were quantified using a Guava easyCyte flow cytometer and InCyte software. Results were expressed as percentages of (CD8+/CD56+/Vγ9+)/Ki67+/IFNγ+ cells over CD8+, CD56+, and Vγ9+ cells.

Statistical analysis

All data are presented as mean ± SD. The results were analyzed by one-way analysis of variance (ANOVA) using GraphPad PRISM software (v.9.4.1, RRID:SCR_002798), where *, $P < 0.05$; **, $P < 0.01$; and ***, $P < 0.001$. Correlation analyses were performed using the non-parametric Spearman Rank Order test, with a cutoff P value of 0.05. The sample size for patient and animal studies was calculated using G*Power software (www.gpower.hhu.de, RRID:SCR_013726), setting $\alpha < 0.05$, $1-\beta = 0.80$, $\rho = 0.30$. According to the median values of ERα (measured by RT-PCR or H score, using as highest and lowest values of the scale ER+ and ER− breast cancers) or PD-L1 (measured by RT-PCR and TPS in NSCLC samples), patients were stratified in lowgroup (ERα/PD-L1 < median value) and highgroup (ERα/PD-L1 ≥ median value). PFS was defined as the time from the start of the treatment to the time of tumor regrowth (in patients) or ≥10% increase in tumor volume in three consecutive measures (in mice). OS was defined as the time from the start of treatment to death. The Kaplan–Meier method was used to calculate OS and PFS. Log-rank test was used to compare the outcomes of each group.

Data availability

The data generated in this study are available upon request from the corresponding author.

Results

ERα level is a strong predictive factor of the response to pembrolizumab in patients with NSCLC

To assess whether sex and hormonal status play a role in the efficacy of IOT, we considered 35 patients with NSCLC who received pembrolizumab as first-line treatment. The percentage of male and female patients with PD, PR, and SD at 6 months was similar (Fig. 1A), and neither PFS nor OS were significantly different (Fig. 1B). All patients had TPS > 50%, but within this group, PD-L1 protein had a distribution ranging from 50% to 100% TPS (Supplementary Table S2). Using TPS and mRNA median values, for this study, we defined patients with PD-L1 < median value as PD-L1low and patients with PD-L1 ≥ median value as PD-L1high. The rationale for this choice was based on previous retrospective observations of better outcomes in extremely high PD-L1 expressors (32, 33). In our cohort, the PD-L1high group, according to the median PD-L1 mRNA, had higher PR + SD (Fig. 1C), higher OS, but not PFS (Fig. 1D), compared with the PD-L1low group. There were no differences between female and male patients in the best response in the PD-L1low group, whereas more PR + SD responses were registered in the PD-L1high female group (Supplementary Fig. S1A). However, no significant changes in PFS and OS were detected between PD-L1high and PD-L1low female or male patients (Supplementary Fig. S1B and S1C). Because neither gender nor PD-L1 status were good predictors of pembrolizumab response, we focused on ERα, because ESR1 (encoding for ERα) emerged as one of the top genes associated with IOT response as a second-third-line treatment (unpublished data). ERαhigh patients, according to the median mRNA value, had better disease control (Fig. 1E), higher PFS and OS (Fig. 1F) than ERαlow patients, even when males and females were considered separately (Supplementary Fig. S1D–S1F). Patients' stratification according to the PD-L1 protein levels, evaluated as immunohistochemical TPS (Supplementary Table S2; Supplementary Fig. S2A), did not show significant differences between PD-L1high and PD-L1low patients in PFS and OS (Fig. 1G). Conversely, based on the H score of ERα protein, ERαhigh patients had significantly better PFS and OS compared with ERαlow patients (Fig. 1H). ERα protein was detected in cancer cells of NSCLC, in cytosol, and in the nucleus (Supplementary Fig. S2B). Intratumor ERα was transcriptionally active: indeed, the mRNA levels of three ERα-target genes, CXCL12, IGFBP4, and ABCA3, were higher in 6 tumors from patients classified as ERαhigh (3 females and 3 males), according to ERα mRNA and protein, compared with 6 tumors classified as ERαlow (Supplementary Fig. S2C).

To validate our data in a larger cohort, we analyzed the LUAD TCGA dataset, where survival did not differ between males and females (Supplementary Fig. S3A). Patients were stratified according to the median value of ESR1 and CD274. In line with the findings of our prospective study, there was no significant difference in OS based on CD274 levels, in whole cohort (Fig. 1I) and in females (Supplementary Fig. S3B). In contrast, ESR1high patients had a significantly better OS than ESR1low patients (Fig. 1J), particularly in females (Supplementary Fig. S3D). In males, high levels of CD274 (Supplementary Fig. S3C) and ESR1 (Supplementary Fig. S3E) were associated with a slightly lower OS. When a coexpression analysis was performed on LUAD TCGA dataset, the phenotype ESR1highCD274high was associated with the best OS, followed by the ESR1highCD274low phenotype. Poor OS characterized ESR1low patients, with the worst scenario represented by ESR1lowCD274high patients (Fig. 1K). Female patients had the same trend (Supplementary Fig. S3F), while in males CD274low phenotypes, either ESR1high or ESR1low, were associated to the best OS (Supplementary Fig. S3G). These data indicate that ESR1 is a strong positive prognostic factor in females and a weak negative prognostic factor in males; CD274 has no meaning in

females and is a weak negative prognostic factor in males. To better understand the linkage between these two partners, we correlated their mRNA levels in each patient of the prospective cohort studied. Unexpectedly, a direct correlation between ERα and PD-L1 expression (Fig. 1L), more significant in females than in males (Supplementary Fig. S3H), was observed. PD-L1 and ERα mRNAs were higher in less advanced stages (Supplementary Fig. S4A–S4D). PD-L1 expression was higher in never-smokers, whereas ERα did not vary with smoking habits (Supplementary Fig. S4E and S4F).

Autocrine 17-β-estradiol/ERα transcriptionally upregulates PD-L1

To deepen the molecular relationships between gender, ERα, and response to anti–PD-1/PD-L1, we screened a panel of 29 commercially available NSCLC cell lines derived from male and female patients with different smoking habits, wild-type or mutated EGFR, derived from primary tumors or metastatic lesions (Supplementary Table S3), recapitulating the clinical features (Supplementary Table S2), and the biological correlations (Supplementary Fig. S5A–S5C) detected in our cohort of patients. There was a positive correlation between the levels of ERα (Fig. 2A) or 17-β-estradiol and the amount of PD-L1 (Fig. 2B), which was more robust in female-derived cell lines.

Next, we focused on the female- and male-derived cell lines with the lowest (NCI-H1385, A549) and highest (NCI-H1975, NCI-H1650) levels of ERα mRNA (Fig. 2C). In all lines, ERβ mRNA varied similarly, but to a lesser extent than ERα (Supplementary Fig. S6A), and the correlation between ERβ and PD-L1 levels was low (Supplementary Fig. S6B), making a causal relationship between ERβ and PD-L1 unlikely. Conversely, ERα protein and its active form phospho(Ser118)ERα (34) were present in nuclear extracts and mirrored mRNA expression (Fig. 2D). ERα was transcriptionally active, as the levels of its target genes varied according to the amount of nuclear ERα/phospho(Ser118)ERα protein (Supplementary Fig. S6C).

Both male- and female-derived cell lines produced 17-β-estradiol (Fig. 2E). This phenomenon was likely of autocrine origin, as suggested by the lack of differences in follicular stimulating hormone receptor (FSHR) and luteinizing hormone receptor (LHR) levels (Supplementary Fig. S7A and S7B) and by the detection of aromatase, whose expression was higher in 17-β-estradiol highly producing cells (Fig. 2F). 17-β-estradiol/ER was the only steroid hormone competent axis in the NSCLC cell lines analyzed: progesterone was homogeneously produced in all the cell lines (Supplementary Fig. S8A), testosterone was higher in male-derived cell lines (Supplementary Fig. S8B), but the production of these hormones was unrelated to the expression of the respective receptors (Supplementary Fig. S8C–S8E).

Consistent with the PD-L1 levels in the whole pool (Fig. 2A and B), PD-L1 on the cell surface followed the same trend as 17-β-estradiol/ERα levels in the four cell lines analyzed: female 17-β-estradiol/ERα highNCI-H1975>male 17-β-estradiol/ERα highNCI-H1650>female 17-β-estradiol/ERα lowNCI-H1385≥male 17-β-estradiol/ERα lowA549 cells (Fig. 2G). Of note, ERα-overexpressing NCI-H1385 cells, characterized by levels of ERα mRNA (Fig. 2C) and active protein (Fig. 2D) comparable with wild-type NCI-H1975, also increased the surface PD-L1 amount as in wild-type NCI-H1975 (Fig. 2G). Conversely, ERα-silenced NCI-H1975 cells (Fig. 2C and D) had a marked reduction in PD-L1 protein (Fig. 2G). The ERα/aromatase-expressing, 17-β-estradiol-producing breast cancer MCF-7 cells (Fig. 2C–F) had the highest amount of surface PD-L1 (Fig. 2G).

Because blocking concentrations (35) of the anti–PD-L1 atezolizumab did not change the nuclear levels of ERα or its phosphorylation (Supplementary Fig. S9), it is unlikely that the activity of PD-L1 modulates ERα.

Conversely, ERα-overexpressing NCI-H1385 cells had PD-L1 mRNA levels comparable with wild-type NCI-H1975 and MCF-7 cells, while in ERα-silenced NCI-H1975 cells, the PD-L1 mRNA was dramatically reduced (Fig. 3A). Scanning of CD274 promoter highlighted the presence of two EREs (Fig. 3B). In NCI-H1385 ERα was poorly bound to ERE1 and ERE2 of CD274 promoter, while the binding was higher in NCI-H1975 and MCF-7 cells. ERα binding was increased and decreased in ERα-overexpressing NCI-H1385 cells and in ERα-silenced NCI-H1975 cells, respectively (Fig. 3C), and was higher in female than in male NSCLC cells (Fig. 3D and E). Notably, the ERα inhibitor fulvestrant and the aromatase inhibitor letrozole, used at clinically achievable concentrations (10 nmol/L; refs. 36, 37), were able to reduce ERα transcriptional activity (Supplementary Fig. S10A) or 17-β-estradiol synthesis (Supplementary Fig. S10B), decreased the binding of ERα to ERE1 and, to a lesser extent, ERE2, on CD274 promoter of 17-β-estradiol/ERα highNCI-H1975 cells (Fig. 3F), decreased PD-L1 mRNA (Fig. 3G), and protein (Fig. 3H). ERβ was transcriptionally less active than ERα (Supplementary Fig. S11).

EGFR downstream effectors phosphorylate ERα and modulate PD-L1 levels

In addition to the binding of 17-β-estradiol, phosphorylation of Ser118 is necessary for the maximal transcriptional efficacy of ERα (34). Because 17-β-estradiol increases the activity of EGFR and downstream effectors ERK1/2 and Akt (38), two kinases activating ERα (39, 40), we evaluated the effects of inhibiting doses of Akt inhibitor MK-2206 (1 μmol/L), ERK1/2 inhibitor U-0126 (10 μmol/L), and EGFR inhibitor AZD9291/osimertinib (1 μmol/L; Supplementary Fig. S12A–S12C). All inhibitors reduced the phosphorylation of ERα at Ser118 (Fig. 4A), even in EGFR-mutated NCI-H1975 and NCI-H1650 cells, where Akt and ERK1/2 were more activated (Fig. 4B). Intriguingly, a direct correlation, stronger in female-derived cell lines, emerged between EGFR kinase activity and ERα phosphorylation at Ser118 (Fig. 4C and D). To prove that ERα phosphorylation was dependent on EGFR activity, we knocked out endogenous EGFR in NCI-H1385 cells, the female-derived cell line with the lowest EGFR activity/ERα phosphorylation, and exogenously expressed the constitutively activated L858R-EGFR present in NCI-H1975 cells (41), the female cell line with the highest EGFR activity/ERα phosphorylation (Supplementary Fig. S13A–S13E). The newly generated EGFR-switched-on activity NCI-H1385 cells displayed the same amount of phospho(S118)ERα (Fig. 4E) and PD-L1 on their surface (Fig. 4F) compared with parental NCI-H1975 cells, suggesting that EGFR downstream signaling upregulates PD-L1 by activating ERα.

Aromatase inhibitor enhances the efficacy of pembrolizumab in ERαhigh xenografts and patient-derived xenografts by relieving the PD-L1–mediated immune-suppression

To investigate whether estrogen-targeting agents could be useful additional agents in IOT protocols, we implanted female-derived NCI-H1385 and NCI-H1975 tumors, and male-derived A549 and NCI-H1650 tumors in Hu-CD34+NSG mice, which have already been used to test the efficacy of anti–PD-1/PD-L1 (42). Notwithstanding the different rates of growth of each line, pembrolizumab reduced tumor growth with higher efficacy in ERα hightumors than in ERα lowtumors (Fig. 5A). Letrozole alone had no effect, but the combination of letrozole and pembrolizumab markedly reduced tumor growth (Fig. 5A), increased PFS and OS (Fig. 5B and C) with this rank of efficacy: female ERα highNCI-H1975 tumors > male ERα highNCI-H1650 and female ERα lowNCI-H1385 tumors > male ERα lowA549 tumors (Fig. 5A). Within each tumor sex, animals bearing ERα hightumors had higher PFS and OS (Fig. 5B and C) in response to pembrolizumab, recapitulating the clinical findings observed in the cohort of patients with NSCLC (Fig. 1). In mice treated with chemo-immuno-therapy (cisplatin + pembrolizumab), we did not observe any gender-related difference (Supplementary Fig. S14): the efficacy of chemo-immuno-therapy was higher in female ERα lowNCI-H1385 and male ERα highNCI-H1650 tumors that were sensitive to cisplatin (31), lower in female ERα highNCI-H1975 tumors and male ERα lowA549 tumors that were resistant (31). The aromatase

inhibitor enhanced chemotherapy efficacy, with the maximal efficacy in ERαhigh tumors of both genders (Supplementary Fig. S14).

Letrozole, alone or in combination with pembrolizumab, reduced the percentage of PD-L1+NSCLC cells in the tumors (Fig. 5D). Both pembrolizumab and letrozole alone slightly increased the amount of activated (IFNγ+) and proliferating (Ki67+) cytotoxic TILs, such as CD8+ T cells, NK cells, and Vγ9Vδ2+ T cells (Fig. 5E–G). These populations were further increased by the letrozole + pembrolizumab combination, with maximal effects in female ERα highNCI-H1975 tumors, followed by male ERα highNCI-H1650 and female ERα lowNCI-H1385 tumors, and finally by male ERα lowA549 tumors (Fig. 5E–G).

Next, we verified if the same trend was recapitulated in immune-PDXs, implanting the cancer cells from the following patients: #10 (female, ERαlow), #3 (female, ERαhigh), #25 (male, ERαlow), #32 (male, ERαhigh; Fig. 6A). Patients #10 and #25 had bad response to IOT, low PFS and OS, while patients #3 and #32 had good response, high PFS and OS (Supplementary Table S2). In the matched immune-PDXs, pembrolizumab, alone or combined with letrozole, showed the maximal efficacy in ERαhigh tumors, the lowest efficacy in ERαlow tumors. Female ERαhigh tumors showed the highest benefit from the combination of letrozole and pembrolizumab, followed by male ERαhigh/female ERαlowtumors; minimal benefits were obtained in male ERαlow tumors (Fig. 6B). Similarly, the combination of pembrolizumab and letrozole reduced the amount of PD-L1 (Fig. 6C) and increased the active infiltrating CD8+ T cells, NK cells, and Vγ9Vδ2+ T cells (Fig. 6D–F). A transcriptome analysis targeted on immune-related genes indicated that female-derived ERαhigh tumors had higher ICP/immune-activating receptors and co-receptors ratio, higher immune-suppressive/immune-activating cytokines ratio, lower expression of IFNγ-dependent genes than female ERαlow tumors. In male-derived tumors, ERαhigh samples had a transcriptome profile similar to females, while ERαlow samples had the lowest expression of both immune-activating and immune-suppressive genes (Fig. 6G). Letrozole, alone and combined with pembrolizumab, reversed the immune-suppressive environment by increasing T-lymphocyte–activating receptors/co-receptors, immune-active/immune-suppressive cytokines ratio and IFNγ-dependent genes. This immune-reshaping was maximal in female ERαhightumors, moderate in female ERαlowtumors and in male ERαhightumors, minimal in male ERαlow tumors (Fig. 6G).

Finally, to investigate whether the effect on tumors and their immune environment was durable, we analyzed different cohorts of animals that, after receiving letrozole + pembrolizumab for 5 weeks, were (i) left untreated; (ii) treated with letrozole alone; (iii) treated with letrozole followed by letrozole + pembrolizumab for an additional 5 weeks. Moving from protocol (i) to (ii) and (iii), we observed a progressively stronger reduction in tumor growth and even a regression with treatment (iii) (Supplementary Fig. S15A), a decrease in tumor PD-L1+ cells explanted at week 15 (Supplementary Fig. S15B), an increase in the amount of activated CD8+ T-lymphocytes, NK cells, and Vγ9Vδ2+ T cells (Supplementary Fig. S15C–S15E). Tumor regression and activation of TILs were dependent on sex and ERα: they were higher in female xenografts (ERα highNCI-H1975 > ERα lowNCI-H1385 tumors) than in male xenografts (ERα highNCI-H1650 > ERα lowA549 tumors).

Discussion

This study demonstrates that estrogen-dependent circuitries are mediators and predictors of response to pembrolizumab, an ICI agent approved for first-line therapy, alone or in combination with chemotherapy, for advanced NSCLC. Indeed, in patients who received pembrolizumab as first-line treatment in

monotherapy, we did not observe significant differences in outcomes between male and female patients, nor between patients stratified on to PD-L1 amount. We cannot exclude the possibility that the lack of strong predictivity may be attributed to the relatively small number of enrolled patients. Alternatively, other factors might better explain the different efficacy of ICIs. Surprisingly, the level of ERα emerged as a strong predictive factor for pembrolizumab efficacy, independent of sex, in our prospective cohort. This observation was supported by the analysis of the larger LUAD TCGA cohort, where high levels of ESR1 represent a positive prognostic factor, high levels of CD274 do not. After disaggregating the internal prospective cohort and the LUAD TCGA dataset according to sex, ESR1 emerged as the main positive prognostic factor in females and as a weak negative prognostic factor in males, while in both the genders, CD274 did not have a significant prognostic value. One limitation of TCGA is the lack of precise information on the number of patients receiving IOT and on the type of treatment (e.g., immunotherapy versus chemo-immunotherapy; immunotherapy as first-line versus immunotherapy as second/third-line treatment). The ROC Plotter Immunotherapy database (https://www.rocplot.org/immune) provided this information, but it did not include studies on NSCLC yet. However, in the large cohort (n = 467) of melanoma patients subjected to anti–PD-1/anti–PD-L1 treatment filed in this database, ESR1 gene was a stronger predictor of response compared with CD274, in line with the results obtained in our prospective cohort. In real patients, ERα and PD-L1 are coexpressed at different amounts, in a continuous manner; analyzing them separately may introduce a bias. The coexpression analyses indicated that ESR1highCD274high phenotype was the most favorable in the LUAD TCGA whole cohort and females, the worst phenotype in males. This complex scenario suggests that only the concurrent evaluation of gender, ESR1/ERα and CD274/PD-L1 levels may provide reliable information; considered singularly, these parameters had uncertain prognostic value.

Interestingly, ERα levels directly correlated with PD-L1 expression, particularly in females, opening the way to investigate whether and how ERα-dependent circuitry may affect PD-L1 expression and response to ICIs. To this aim, 29 NSCLC cell lines, taking into consideration combinations of sex (10 females, 19 males), primary (20) or metastatic (8) localizations, smoking habits (18 smokers), and EGFR mutations (23 wild-type, 6 mutated) that accurately recapitulated the patient cohort analyzed (15 females, 20 males; 24 primary, 11 metastatic localizations; 32 current or former smokers) were selected. The screening analysis of these NSCLC cell lines excluded gender-, smoke-, and stage-dependent differences in PD-L1 expression, but it confirmed a direct correlation between ERα expression/17-β-estradiol levels and PD-L1 levels, stronger in cells derived from females where ERα levels were generally higher. In addition, the analysis of the cell line pool highlighted different scenarios existing in NSCLC, ranging from 17-β-estradiol/ERα hightumors to 17-β-estradiol/ERα lowtumors: female- and primary tumor-derived NSCLC models mostly belong to the first category, male- and metastatic-derived cell lines are mainly included in the second category.

Mechanistically, the complex 17-β-estradiol/ERα is a transcriptional inducer of PD-L1, as demonstrated by the effects of ERα overexpression and silencing on PD-L1 expression. A high expression of PD-L1 is associated with higher response rate to ICIs in NSCLC (32). Based on these observations, female-derived NSCLC tumors, characterized by a higher percentage of 17-β-estradiol/ERα/PD-L1 highcells, should benefit more from pembrolizumab treatment, confirming the clinical studies reporting a higher benefit of IOT in women (6, 7). On the other hand, a small percentage of NSCLC cells derived from males also had a 17-β-estradiol/ERα/PD-L1 highphenotype, and a small percentage of female-derived cells had the 17-β-estradiol/ERα/PD-L1 lowphenotype, common with most male-derived NSCLC cells. This intricate biological scenario explains why other retrospective studies reported a higher benefit of IOT in males (2–5), or the absence of any gender-dependent benefits (1, 8, 9). Our experimental data suggest that, beyond sex, 17-β-estradiol/ERα levels must be evaluated as predictors of IOT benefit, because they finely regulate PD-L1 expression in NSCLC.

The amount of active (i.e., nuclear and phosphorylated) ERα was independent of sex, but its transcriptional activity on CD274 promoter was higher in female-derived cells. This is not surprising because female-derived NSCLC cells are more responsive to 17-β-estradiol and activate ER-transcriptional programs more than male-derived NSCLC cells, according to the higher expression of ER coactivators (43). ERβ, which is more frequently detected in the nucleus of NSCLC biopsies than ERα (16) and regulates the transcription of a broader spectrum of genes (44), is the most prominent isoform of ER involved in NSCLC pathogenesis and progression (19). However, in the case of CD274 upregulation, ERα plays a predominant role.

The presence of 17-β-estradiol and the phosphorylation on Ser118 make ERα transcriptionally active. The lung is rich in estrogen-synthesizing enzymes (45), particularly aromatase, which correlates with ER levels and is expressed in both male and female patients of premenopausal and postmenopausal age (45). We detected aromatase in both female- and male-derived NSCLC cells. 17-β-estradiol levels varied according to aromatase levels but were not correlated with FSHR/LHR. These findings, together with the effective decrease in 17-β-estradiol levels in letrozole-treated cells, support the hypothesis that NSCLC cells have an autocrine production of estrogens, independent of ovarian activity, age, or sex.

As far as phosphorylation on Ser118 is concerned, the use of selective inhibitors of EGFR and the downstream kinases Akt and ERK1/2 indicated that the EGFR/Akt and EGFR/ERK1/2 axes control the phosphorylation of ERα and consequently the levels of PD-L1. The strong correlation between EGFR activity and phospho(Ser118)-ERα supports this hypothesis. In addition, by switching on the activity of EGFR in the cell line with the lowest EGFR activity and overexpressing a constitutively active receptor, we increased the phosphorylation of ERα and the amount of PD-L1 to the same level of the cell line with the highest endogenous activity of EGFR. These data explain why the introduction of exogenous EGFR-carrying driver mutations upregulated PD-L1 in the bronchial epithelium (46). Although mutated EGFR is usually associated with higher tyrosine kinase activity, EGFR mutations do not correlate well with PD-L1 expression in patients with NSCLC (47). Instead, the phosphorylation activity of EGFR has a more robust correlation with PD-L1 levels (47), in line with our findings. The originality of the current work relies on the demonstration that ERα is the missing ring between EGFR and PD-L1. Overall, we propose a four-biomarker–based signature, EGFR activity, 17-β-estradiol production, ESR1/ERα, and CD274/PD-L1 coexpression levels, which may predict the response to pembrolizumab and may help to select patients who will obtain the highest benefit from ICI and antiestrogen agent combination.

Indeed, the control of PD-L1 by the 17-β-estradiol/ERα complex offers an opportunity to explore the use of antiestrogens or aromatase inhibitors in IOT protocols. Both fulvestrant and anastrazole have been safely tested in phase I/II trials in combination with chemotherapy or EGFR inhibitors (19, 48); however, their association with IOT has not been investigated. Here, we explored a platform of humanized mice to test the association between pembrolizumab and letrozole in NSCLC xenografts and PDXs. In both cases, the combination of these drugs reduced tumor growth, particularly in female-derived tumors with a 17-β-estradiol/ERα highphenotype. Conversely, a marginal benefit was observed in male patients with a 17-β-estradiol/ERα lowphenotype. Tumors of both sexes with a 17-β-estradiol/ERα intermediatephenotype had a moderate benefit. Being characterized by higher estrogen production and ERα levels, female-derived tumors have a higher benefit from the combination of ICI and antiestrogen agents in terms of tumor reduction, OS and PFS compared with male-derived tumors. Although small, this platform of humanized PDX was functional to identify, between patient responder and non-responder to first-line IOT, those who

may benefit from anti-estrogen agents as immune-sensitizers. Interestingly, beyond increasing the efficacy of IOT, letrozole also increases the efficacy of chemo-immuno-therapy. Also in this setting, the maximal benefit was dependent on ERα levels, resulting maximal in ERα high tumors, and was independent from the gender.

In line with in vitro setting, letrozole downregulated PD-L1 expression in the tumors. Although a decrease in PD-L1 expression is a sign of acquired resistance to pembrolizumab (49), the most prominent effect of the letrozole + pembrolizumab combination is the relief of tumor-induced immunosuppression, with increased efficacy of pembrolizumab in long-term experiments. Indeed, in responsive tumors, the combination of letrozole and pembrolizumab increased the number of active CD8+ T-lymphocytes and NK cells, two antitumor populations whose expansion is an index of ICI efficacy (42, 45, 50). The increase in proliferation and activation of Vγ9Vδ2+ T cells was a third factor determining durable immune control of tumor growth. Indeed, γδ T cells are the most favorable prognostic tumor-infiltrating subpopulations in solid cancers, including lung adenocarcinomas (51). In a previous study, PD-L1 mRNA was weakly associated with the number of TILs in 35 patients with NSCLC subjected to anti–PD-1/anti–PD-L1 treatment, and was among the 730 genes (GSE93157) related to CD4+/CD8+ T-lymphocytes, NK cells and IFN-dependent pathways associated with good PFS (52). ERα was not included in this gene set. To the best of our knowledge, the current work is the first one highlighting that a high activity of 17-β-estradiol/ERα axis is associated with high levels of PD-L1, and that aromatase inhibitors increase the number and activity of infiltrating effector cells. This beneficial imprinting on the immune environment was the “deus ex machina” that explains the benefits of prolonged treatment with letrozole. Indeed, while a 5-week treatment with pembrolizumab and letrozole only delayed tumor growth, the continuous administration of letrozole after this first cycle produced long-term tumor control that became an even deeper regression in animals treated with a second cycle of the combination therapy. The high efficacy of this protocol was likely due to the durable reactivation of antitumor TILs induced by the aromatase inhibitor, an event that may sensitize the tumors to a second exposure to ICI. As expected, the benefit was greater in female-derived tumors, in which 17-β-estradiol and ERα levels were higher. In males, the benefit was proportional to the intratumor amount of estrogen and ERα. Estrogens play a key role in modulating the immune environment toward immunosuppression: in ER+ breast cancers, 17-β-estradiol strongly inhibits the cytotoxic functions of CD8+T-lymphocytes and NK cells, whereas aromatase inhibitors increase TILs, a feature associated with improved OS (15). In NSCLC xenografts, letrozole increased IFNγ signaling pathway, receptor/coreceptors and soluble mediators increasing T-lymphocyte activity, and reduced ICP levels. The shift from an immunosuppressive toward an immune-active microenvironment was maximal in ERαhigh tumors, particularly of female patients. This subgroup may have the highest benefit from the combination of IOT with antiestrogen agents.

In conclusion, this work demonstrates that 17-β-estradiol production and ERα activity, controlled by EGFR downstream signaling, upregulate PD-L1 expression and influence the response to anti–PD-1/PD-L1 agents in NSCLC. Because high levels of 17-β-estradiol and ERα are more common in female-derived tumors, females may benefit more from IOT than males, but high intratumor levels of 17-β-estradiol and ERα determine the same response to pembrolizumab in males (Supplementary Fig. S16). Aromatase inhibitors should be explored as possible enhancers of ICIs, due to the reduction of PD-L1 and consequent relief of tumor-induced immune suppression, with different benefits depending on the 17-β-estradiol/ERα status. The routine assessment of 17-β-estradiol and coexpressed ERα/PD-L1 in NSCLC samples may represent a new stratification process to predict the response to IOT and identify patients who can benefit from the inclusion of aromatase inhibitors in association with ICI.

Acknowledgments

This work was supported by the Italian Association of Cancer Research (AIRC; IG21408 to C. Riganti, IG23760 to G.V. Scagliotti), the Cassa di Risparmio Foundation, Torino, Italy (ID 2018.0568 and ID2021.05556 to C. Riganti), Compagnia di San Paolo Funding 2021 (to C. Riganti), and the European Cooperation in Science and Technology (COST; CA17104 and IG17104 to C. Riganti). We thank Costanzo Costamagna for the technical assistance.

The publication costs of this article were defrayed in part by the payment of publication fees. Therefore, and solely to indicate this fact, this article is hereby marked “advertisement” in accordance with 18 USC section 1734.

References

1. Dafni U , Tsourti Z , Vervita K , Peters S . Immune checkpoint inhibitors, alone or in combination with chemotherapy, as first-line treatment for advanced non-small cell lung cancer. a systematic review and network meta-analysis. Lung Cancer 2019;134:127–40.

2. Grassadonia A , Sperduti I , Vici P , Iezzi L , Brocco D , Gamucci T , et al. Effect of gender on the outcome of patients receiving immune checkpoint inhibitors for advanced cancer: a systematic review and meta-analysis of phase III randomized clinical trials. J Clin Med 2018;7:542.

3. Conforti F , Pala L , Bagnardi V , De Pas T , Martinetti M , Viale G , et al. Cancer immunotherapy efficacy and patients' sex: a systematic review and meta-analysis. Lancet Oncol 2018;19:737–46.

4. Wallis CJD , Butaney M , Satkunasivam R , Freedland SJ , Patel SP , Hamid O , et al. Association of patient sex with efficacy of immune checkpoint inhibitors and overall survival in advanced cancers: a systematic review and meta-analysis. JAMA Oncol 2019;5:529–36.

5. Wang C , Qiao W , Jiang Y , Zhu M , Shao J , Ren P , et al. Effect of sex on the efficacy of patients receiving immune checkpoint inhibitors in advanced non-small cell lung cancer. Cancer Med 2019;8:4023–31.

6. Gandhi L , Rodríguez-Abreu D , Gadgeel S , Esteban E , Felip E , De Angelis F , et al. Pembrolizumab plus chemotherapy in metastatic non-small-cell lung cancer. N Engl J Med 2018;378:2078–92.

7. Socinski MA , Jotte RM , Cappuzzo F , Orlandi F , Stroyakovskiy D , Nogami N , et al. Atezolizumab for first-line treatment of metastatic nonsquamous NSCLC. N Engl J Med 2018;378:2288–301.

8. Reck M , Rodríguez-Abreu D , Robinson AG , Hui R , Csőszi T , Fülöp A , et al. Pembrolizumab versus chemotherapy for PD-L1-positive non-small-cell lung cancer. N Engl J Med 2016;375:1823–33.

9. Rittmeyer A , Barlesi F , Waterkamp D , Park K , Ciardiello F , von Pawel J , et al. Atezolizumab versus docetaxel in patients with previously treated non-small-cell lung cancer (OAK): a phase 3, open-label, multicentre randomised controlled trial. Lancet 2017;389:255–65.

10. Li CH , Haider S , Shiah YJ , Thai K , Boutros PC . Sex differences in cancer driver genes and biomarkers. Cancer Res 2018;78:5527–37.

11. Vavalà T , Catino A , Pizzutilo P , Longo V , Galetta D . Gender differences and immunotherapy outcome in advanced lung cancer. Int J Mol Sci 2021;22:11942.

12. Lopes-Ramos CM , Kuijjer ML , Ogino S , Fuchs CS , DeMeo DL , Glass K , et al. Gene regulatory network analysis identifies sex-linked differences in colon cancer drug metabolism. Cancer Res 2018;78:5538–47.

13. Clocchiatti A , Cora E , Zhang Y , Dotto GP . Sexual dimorphism in cancer. Nat Rev Cancer 2016;16:330–9.

14. Rothenberger NJ , Somasundaram A , Stabile LP . The role of the estrogen pathway in the tumor microenvironment. Int J Mol Sci 2018;19:611.

15. Frega S , Dal Maso A , Ferro A , Bonanno L , Conte P , Pasello G . Heterogeneous tumor features and treatment outcome between males and females with lung cancer (LC): do gender and sex matter? Crit Rev Oncol Hematol 2019;138:87–103.

16. Smida T , Bruno TC , Stabile LP . Influence of estrogen on the NSCLC microenvironment: a comprehensive picture and clinical implications. Front Oncol 2020;10:137.

17. Kawai H , Ishii A , Washiya K , Konno T , Kon H , Yamaya C , et al. Estrogen receptor alpha and beta are prognostic factors in non-small cell lung cancer. Clin Cancer Res 2005;11:5084–9.

18. Li W , Tse LA , Wang F . Prognostic value of estrogen receptors mRNA expression in non-small cell lung cancer: a systematic review and meta-analysis. Steroids 2015;104:129–36.

19. Berardi R , Morgese F , Santinelli A , Onofri A , Biscotti T , Brunelli A , et al. Hormonal receptors in lung adenocarcinoma: expression and difference in outcome by sex. Oncotarget 2016;7:82648–57.

20. Kazmi N , Márquez-Garbán DC , Aivazyan L , Hamilton N , Garon EB , Goodglick L , et al. The role of estrogen, progesterone and aromatase in human non-small-cell lung cancer. Lung Cancer Manag 2012;1:259–72.

21. Rodriguez-Lara V , Hernandez-Martinez JM , Arrieta O . Influence of estrogen in non-small cell lung cancer and its clinical implications. J Thorac Dis 2018;10:482–97.

22. Zhao XZ , Liu Y , Zhou LJ , Wang ZQ , Wu ZH , Yang XY . Role of estrogen in lung cancer based on the estrogen receptor-epithelial mesenchymal transduction signaling pathways. Onco Targets Ther 2015;8:2849–63.

23. Grott M , Karakaya S , Mayer F , Baertling F , Beyer C , Kipp M , et al. Progesterone and estrogen prevent cisplatin-induced apoptosis of lung cancer cells. Anticancer Res 2013;33:791–800.

24. Wang Z , Li Z , Ding X , Shen Z , Liu Z , An T , et al. ERβ localization influenced outcomes of EGFR-TKI treatment in NSCLC patients with EGFR mutations. Sci Rep 2015;5:11392.

25. Siegfried JM , Gubish CT , Rothstein ME , Henry C , Stabile LP . Combining the multitargeted tyrosine kinase inhibitor vandetanib with the antiestrogen fulvestrant enhances its antitumor effect in non-small cell lung cancer. J Thorac Oncol 2012;7:485–95.

26. Hua W , Huang X , Li J , Feng W , Sun Y , Guo C . 2-methoxyestradiol inhibits melanoma cell growth by activating adaptive immunity. Immunopharmacol Immunotoxicol 2022;44:541–47.

27. Márquez-Garbán DC , Deng G , Comin-Anduix B , Garcia AJ , Xing Y , Chen HW , et al. Antiestrogens in combination with immune checkpoint inhibitors in breast cancer immunotherapy. J Steroid Biochem Mol Biol 2019;193:105415.

28. Svoronos N , Perales-Puchalt A , Allegrezza MJ , Rutkowski MR , Payne KK , Tesone AJ , et al. Tumor cell-independent estrogen signaling drives disease progression through mobilization of myeloid-derived suppressor cells. Cancer Discov 2017;7:72–85.

29. Righi L , Papotti MG , Ceppi P , Billè A , Bacillo E , Molinaro L , et al. Thymidylate synthase but not excision repair cross-complementation group 1 tumor expression predicts outcome in patients with malignant pleural mesothelioma treated with pemetrexed-based chemotherapy. J Clin Oncol 2010;28:1534–9.

30. Campia I , Sala V , Kopecka J , Leo C , Mitro N , Costamagna C , et al. Digoxin and ouabain induce the efflux of cholesterol via liver X receptor signalling and the synthesis of ATP in cardiomyocytes. Biochem J 2012;447:301–11.

31. Salaroglio IC , Belisario DC , Akman M , La Vecchia S , Godel M , Anobile DP , et al. Mitochondrial ROS drive resistance to chemotherapy and immune-killing in hypoxic non-small cell lung cancer. J Exp Clin Cancer Res 2022;41:243.

32. Aguilar EJ , Ricciuti B , Gainor JF , Kehl KL , Kravets S , Dahlberg S , et al. Outcomes to first-line pembrolizumab in patients with non-small-cell lung cancer and very high PD-L1 expression. Ann Oncol 2019;30:1653–59.

33. Sezer A , Kilickap S , Gümüş M , Bondarenko I , Özgüroğlu M , Gogishvili M , et al. Cemiplimab monotherapy for first-line treatment of advanced non-small-cell lung cancer with PD-L1 of at least 50%: a multicentre, open-label, global, phase 3, randomised, controlled trial. Lancet 2021;397:592–604.

34. Weitsman GE , Li L , Skliris GP , Davie JR , Ung K , Niu Y , et al. Estrogen receptor-alpha phosphorylated at Ser118 is present at the promoters of estrogen-regulated genes and is not altered due to HER-2 overexpression. Cancer Res 2006;66:10162–70.

35. Inman BA , Longo TA , Ramalingam S , Harrison MR . Atezolizumab: a PD-L1-blocking antibody for bladder cancer. Clin Cancer Res 2017;23:1886–90.

36. Robertson JF , Erikstein B , Osborne KC , Pippen J , Come SE , Parker LM , et al. Pharmacokinetic profile of intramuscular fulvestrant in advanced breast cancer. Clin Pharmacokinet 2004;43:529–38.

37. Desta Z , Kreutz Y , Nguyen AT , Li L , Skaar T , Kamdem LK , et al. Plasma letrozole concentrations in postmenopausal women with breast cancer are associated with CYP2A6 genetic variants, body mass index, and age. Clin Pharmacol Ther 2011;90:693–700.

38. Choi YA , Koo JS , Park JS , Park MY , Jeong AL , Oh KS , et al. Estradiol enhances CIP2A expression by the activation of p70 S6 kinase. Endocr Relat Cancer 2014;21:189–202.

39. Stabile LP , Lyker JS , Gubish CT , Zhang W , Grandis JR , Siegfried JM . Combined targeting of the estrogen receptor and the epidermal growth factor receptor in non-small cell lung cancer shows enhanced antiproliferative effects. Cancer Res 2005;65:1459–70.

40. Moerkens M , Zhang Y , Wester L , van de Water B , Meerman JH . Epidermal growth factor receptor signalling in human breast cancer cells operates parallel to estrogen receptor α signalling and results in tamoxifen insensitive proliferation. BMC Cancer 2014;14:283.

41. Sordella R , Bell DW , Haber DA , Settleman J . Gefitinib-sensitizing EGFR mutations in lung cancer activate anti-apoptotic pathways. Science 2004;305:1163–7.

42. Capasso A , Lang J , Pitts TM , Jordan KR , Lieu CH , Davis SL , et al. Characterization of immune responses to anti-PD-1 mono and combination immunotherapy in hematopoietic humanized mice implanted with tumor xenografts. J Immunother Cancer 2019;7:37.

43. Kerr A II , Eliason JF , Wittliff JL . Steroid receptor and growth factor receptor expression in human non small cell lung cancers using cells procured by laser-capture microdissection. Adv Exp Med Biol 2008;617:377–84.

44. Konings GFJ , Reynaert NL , Delvoux B , Verhamme FM , Bracke KR , Brusselle GG , et al. Increased levels of enzymes involved in local estradiol synthesis in chronic obstructive pulmonary disease. Mol Cell Endocrinol 2017;443:23–31.

45. Mah V , Seligson DB , Li A , Márquez DC , Wistuba II , Elshimali Y , et al. Aromatase expression predicts survival in women with early-stage non small cell lung cancer. Cancer Res 2007;67:10484–90.

46. Akbay EA , Koyama S , Carretero J , Altabef A , Tchaicha JH , Christensen CL , et al. Activation of the PD-1 pathway contributes to immune escape in EGFR-driven lung tumors. Cancer Discov 2013;3:1355–63.

47. Suda K , Rozeboom L , Furugaki K , Yu H , Melnick MAC , Ellison K , et al. Increased EGFR phosphorylation correlates with higher programmed death ligand-1 expression: analysis of TKI-resistant lung cancer cell lines. Biomed Res Int 2017;2017:7694202.

48. Garon EB , Siegfried JM , Stabile LP , Young PA , Marquez-Garban DC , Park DJ , et al. Randomized phase II study of fulvestrant and erlotinib compared with erlotinib alone in patients with advanced or metastatic non-small cell lung cancer. Lung Cancer 2018;123:91–98.

49. Takahashi T , Tateishi A , Bychkov A , Fukuoka J . Remarkable alteration of PD-L1 expression after immune checkpoint therapy in patients with non-small-cell lung cancer: two autopsy case reports. Int J Mol Sci 2019;20:2578.

50. Choi B , Lee JS , Kim SJ , Hong D , Park JB , Lee KY . Anti-tumor effects of anti-PD-1 antibody, pembrolizumab, in humanized NSG PDX mice xenografted with dedifferentiated liposarcoma. Cancer Lett 2020;478:56–69.

51. Gentles AJ , Newman AM , Liu CL , Bratman SV , Feng W , Kim D , et al. The prognostic landscape of genes and infiltrating immune cells across human cancers. Nat Med 2015;21:938–45.

52. Prat A , Navarro A , Paré L , Reguart N , Galván P , Pascual T , et al. Immune-related gene expression profiling after PD-1 blockade in non-small cell lung carcinoma, head and neck squamous cell carcinoma, and melanoma. Cancer Res 2017;77:3540–50.

Fig.1

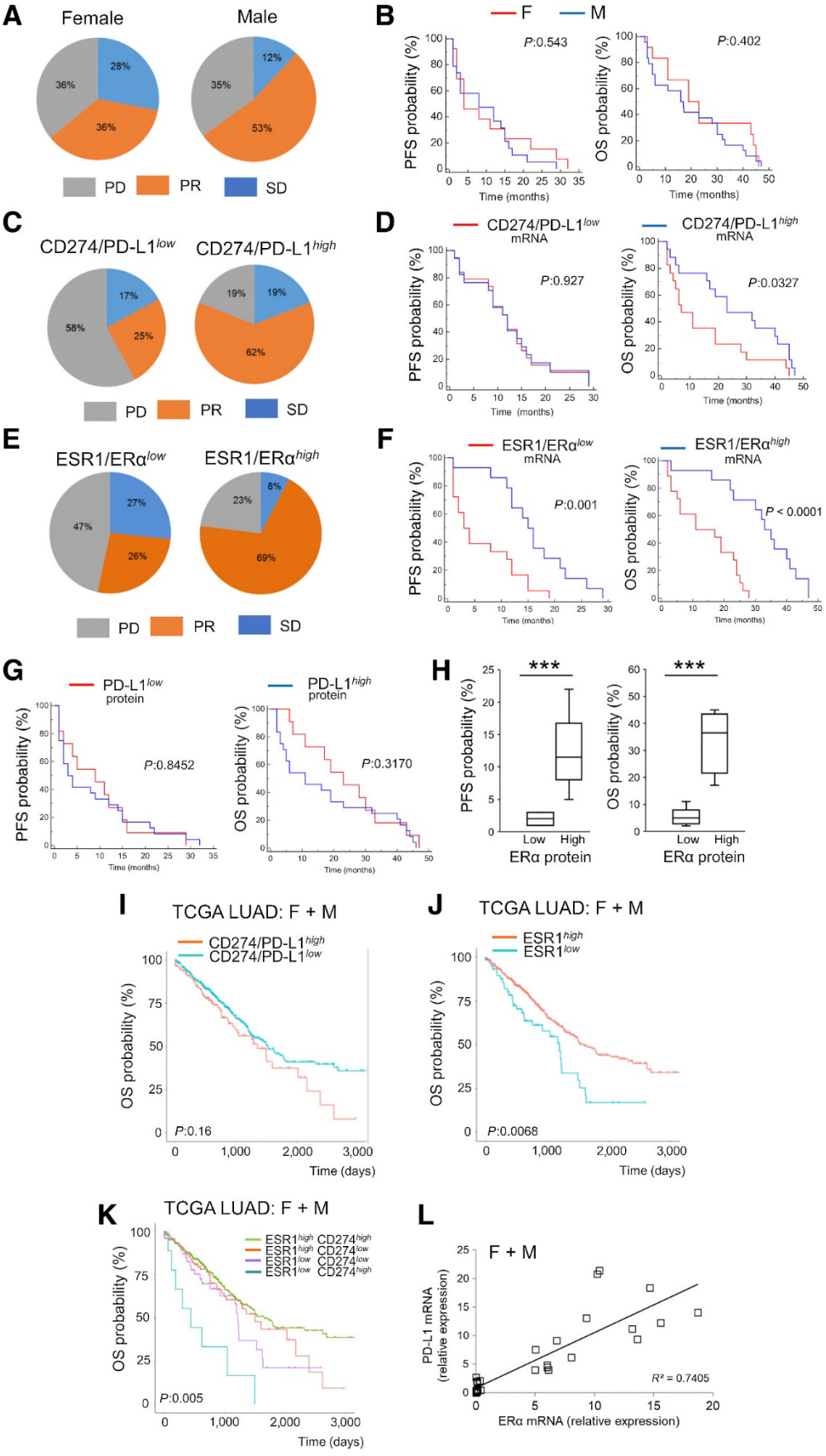
A
Female
Male
28%
36%
36%
12%
35%
53%
PD
PR
SD
B
F
M
P:0.543
P:0.402
PFS probability (%)
OS probability (%)
Time (months)
C
CD274/PD-L1low
CD274/PD-L1high
17%
58%
25%
19%
19%
62%
D
CD274/PD-L1low mRNA
CD274/PD-L1high mRNA
P:0.927
P:0.0327
E
ESR1/ERαlow
ESR1/ERαhigh
27%
47%
26%
8%
23%
69%
F
ESR1/ERαlow mRNA
ESR1/ERαhigh mRNA
P:0.001
P < 0.0001
G
PD-L1low protein
PD-L1high protein
P:0.8452
P:0.3170
H
***
***
Low
High
ERα protein
I
TCGA LUAD: F + M
CD274/PD-L1high
CD274/PD-L1low
P:0.16
Time (days)
J
TCGA LUAD: F + M
ESR1high
ESR1low
P:0.0068
K
TCGA LUAD: F + M
ESR1high CD274high
ESR1high CD274low
ESR1low CD274low
ESR1low CD274high
P:0.005
L
F + M
PD-L1 mRNA (relative expression)
ERα mRNA (relative expression)
R² = 0.7405

ERα expression is a predictive factor of the response to pembrolizumab in patients with NSCLC. Best response (PD, progressive disease; PR, partial response; SD, stable disease) 6 months after the beginning of pembrolizumab treatment as first-line monotherapy, PFS, and OS (Kaplan–Meier and log-rank tests) were analyzed in 35 patients with NSCLC (15 females: F; 20 males: M). A and B, Best response, PFS, and OS in female and male patients. C and D, Best response, PFS, and OS in patients stratified according to the median values of CD274/PD-L1 mRNA measured by RT-PCR (technical triplicates) in the tumor samples. E and F, Best response, PFS, and OS in patients stratified according to the median values of ESR1/ERα mRNA measured by RT-PCR (technical triplicates) in the tumor samples. Median ERα value was calculated using ER+ and ER− breast cancers as highest and lowest values of the scale. G, PFS and OS in PD-L1low versus PD-L1high patients stratified according to the median values of PD-L1 protein, evaluated by immunohistochemical analysis (TPS score, Supplementary Table S2). H, Mean PFS and OS of 6 patients (3 females and 3 males) classified as ERαhigh and ERαlow according to immunohistochemical analysis (H score; Supplementary Fig. S2B). Median ERα value was calculated using ER+ and ER− breast cancers as highest and lowest values of the scale. ***, $P < 0.001$: ERαhigh versus ERαlow tumors. I and J, OS in CD274/PD-L1low versus CD274/PD-L1high patients, and in ESR1/ERαlow versus ESR1/ERαhigh patients of LUAD TGCA, stratified according to the median expression value of the respective genes. K, OS of LUAD TCGA patients, stratified according to the coexpression phenotypes: CD274high/ESR1high, CD274high/ESR1low, CD274low/ESR1high, CD274low/ESR1low. L, Expression of ERα mRNA plotted versus PD-L1 mRNA, both measured by RT-PCR (technical triplicates) in tumor samples.

Fig.2

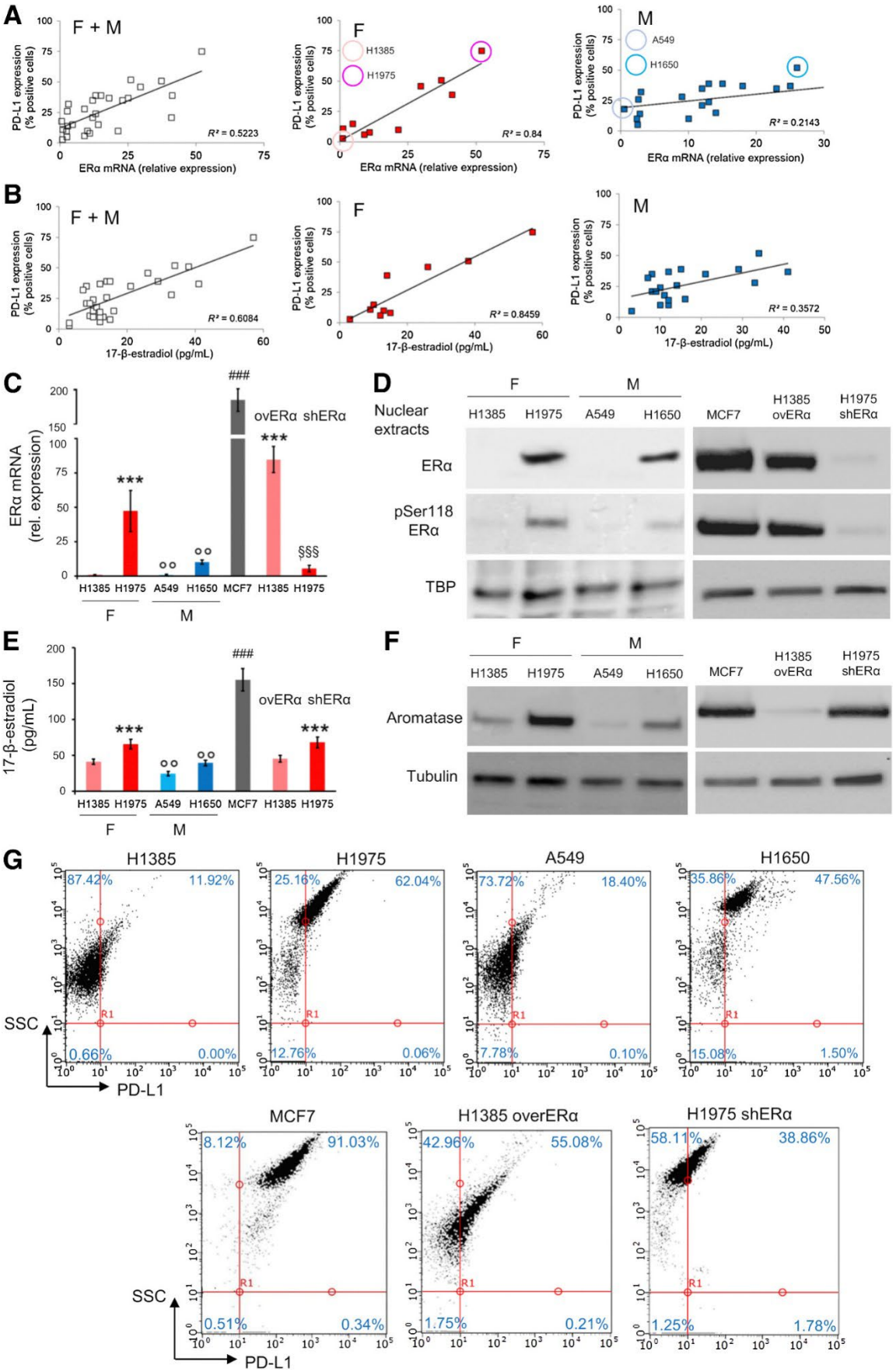
A
F + M
PD-L1 expression (% positive cells)
ERα mRNA (relative expression)
R² = 0.5223
F
H1385
H1975
R² = 0.84
M
A549
H1650
R² = 0.2143
B
F + M
17-β-estradiol (pg/mL)
R² = 0.6084
R² = 0.8459
R² = 0.3572
C
ERα mRNA (rel. expression)
ovERα shERα
###
***
§§§
H1385 H1975 A549 H1650 MCF7 H1385 H1975
F
M
D
Nuclear extracts
ERα
pSer118 ERα
TBP
MCF7
H1385 ovERα
H1975 shERα
E
17-β-estradiol (pg/mL)
F
Aromatase
Tubulin
G
H1385
H1975
A549
H1650
87.42%
11.92%
0.66%
0.00%
25.16%
62.04%
12.76%
0.06%
73.72%
18.40%
7.78%
0.10%
35.86%
47.56%
15.08%
1.50%
SSC
PD-L1
R1
MCF7
H1385 overERα
H1975 shERα
8.12%
91.03%
0.51%
0.34%
42.96%
55.08%
1.75%
0.21%
58.11%
38.86%
1.25%
1.78%

ERα, 17-β-estradiol, and PD-L1 levels in human NSCLC cell lines. A, Expression of ERα mRNA, measured by RT-PCR (technical triplicates), plotted versus expression of surface PD-L1, measured by flow cytometry (technical triplicates), in 29 human NSCLC cell lines derived from female (F) or male (M) patients. B, Levels of 17-β-estradiol, measured by ELISA (technical triplicates), plotted versus the expression of surface PD-L1, measured by flow cytometry (technical triplicates), in 29 human NSCLC cell lines derived from F or M patients. C, ERα mRNA, measured by RT-PCR (technical triplicates), in F-derived NCI-H1385 and NCI-H1975 cells, M-derived A549 and NCI-H1650 cells, ERα-overexpressing NCI-H1385 cells, ERα-silenced NCI-H1975 cells, and breast cancer MCF-7 cells (included as control of ERα/aromatase-expressing, 17-β-estradiol–producing cell line). The relative expression of ERα in wild-type NCI-H1385 cells was 1. Data, mean ± SD (n = 4, biological replicates). ***, $P < 0.001$: NCI-H1975 versus NCI-H1385 cells, overERαNCI-H1385 cells versus wild-type NCI-H1385 cells; §§§, $P < 0.001$: shERαNCI-H1975 cells versus wild-type NCI-H1975 cells; °°, $P < 0.01$: M-derived cells versus mean of F-derived cells; ###, $P < 0.001$: MCF-7 cells versus all the other cell lines (ANOVA). D, Immunoblotting of the indicated proteins in nuclear extracts. TBP was used as a control for equal protein loading. The image is representative of one of three experiments. E, Levels of 17-β-estradiol, measured by ELISA (technical triplicate). Data, mean ± SD (n = 3, biological replicates). ***, $P < 0.01$: NCI-H1975 and shERαNCI-H1975 versus wild-type NCI-H1385 cells; °°, $P < 0.01$: M-derived cells versus mean of F-derived cells; ###$P < 0.001$: MCF-7 cells versus all the other cell lines (ANOVA). F, Immunoblot of aromatase in whole-cell extracts. Tubulin was used as a control for equal protein loading. The image is representative of one of three experiments. G, Surface PD-L1 expression was measured using flow cytometry (technical triplicate). The dot plots are representative of one of four experiments. Percentages indicate positive cells in each quadrant. SSC: side-scatter.

Fig.3

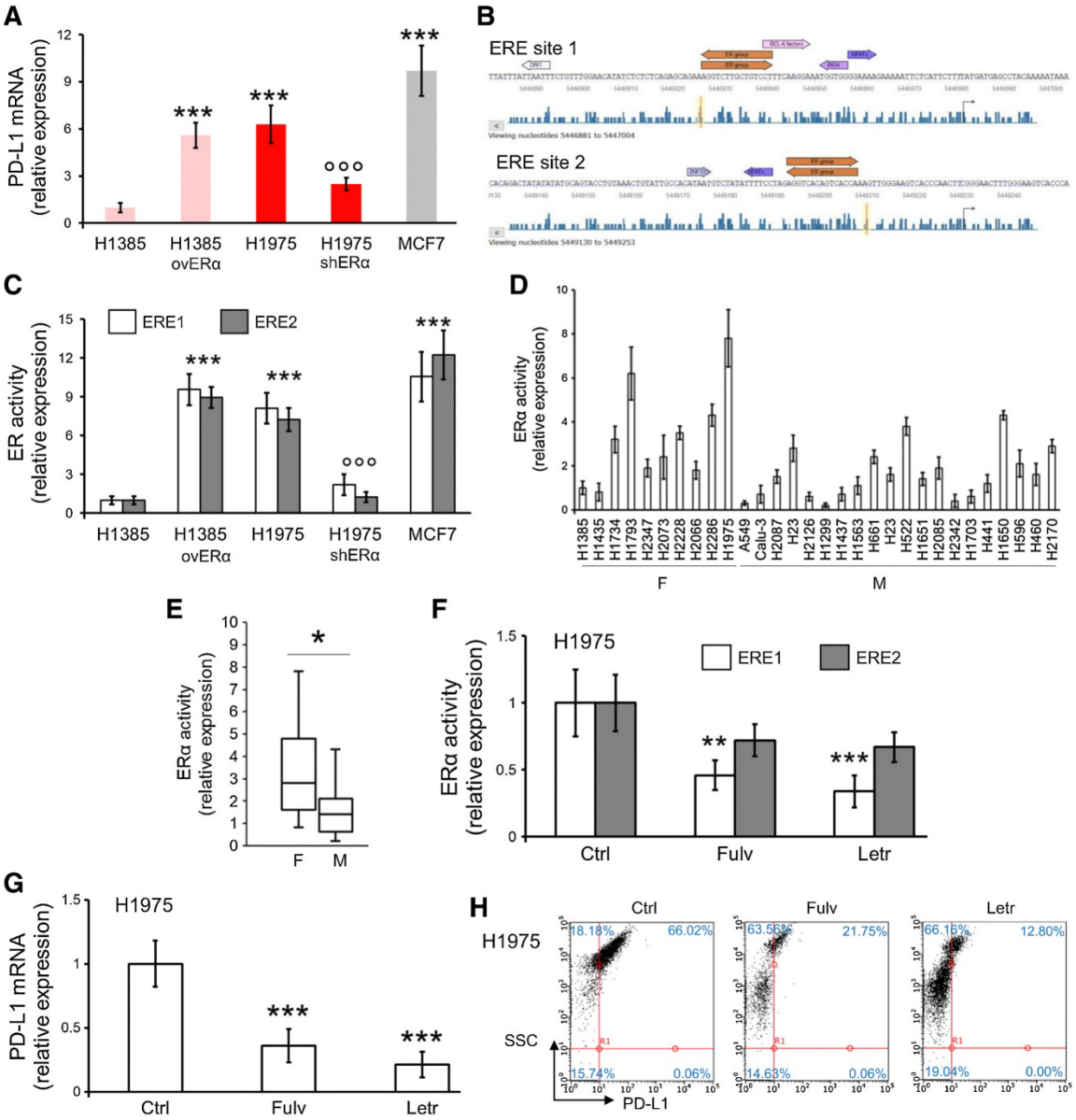

PD-L1 is transcriptionally upregulated by ERα. A, PD-L1 mRNA, measured by RT-PCR (technical triplicate), in NCI-H1385 cells, ERα-overexpressing NCI-H1385 cells, NCI-H1975 cells, ERα-silenced NCI-H1975 cells, breast cancer MCF-7 cells (included as control of ERα/aromatase-expressing, 17-β-estradiol-producing cell line). The relative expression of PD-L1 in wild-type NCI-H1385 cells was 1. Data, mean ± SD (n = 3). ***, P < 0.001: NCI-H1975/overERαNCI-H1385/MCF-7 cells versus wild-type NCI-H1385; °°°, P < 0.001: shERαNCI-H1975 cells versus wild-type NCI-H1975 cells. B, Mapping of ERE1 and ERE2 sites on CD274/PD-L1 promoter (TRANSFAC database). C, Chromatin immunoprecipitation of the ERE1 and ERE2 regions from CD274/PD-L1 promoter using an anti-ERα antibody, followed by RT-PCR of the precipitated products. The activity in NCI-H1385 cells was considered 1. Data, mean ± SD (n = 3, biological replicates). ***, P < 0.001: NCI-H1975/overERαNCI-H1385/MCF-7 cells versus wild-type NCI-H1385; °°°, P < 0.01: shERαNCI-H1975 cells versus wild-type NCI-H1975 cells. D, Chromatin immunoprecipitation of ERE1 from CD274/PD-L1 promoter, followed by RT-PCR of the precipitated products in 29 human NSCLC cell lines derived from female (F) or male (M) patients. Data, mean ± SD (n = 3, biological replicates). The activity of NCI-H1385 cells was considered 1. E, Data of D, pooled for F and M patients. *, P < 0.05: F vs. M (ANOVA). F, NCI-H1975 cells were grown for 24 hours in fresh medium (Ctrl) or in medium containing 10 nmol/L fulvestrant (Fulv), an ERα inhibitor, or 10 nmol/L letrozole (Letr), an aromatase inhibitor. Chromatin immunoprecipitation of the ERE1 and ERE2 regions from CD274/PD-L1 promoter. Data, mean ± SD (n = 3, biological replicates). **, P < 0.01; ***, P < 0.001: Fulv/Letr-treated cells versus Ctrl cells (ANOVA). G, PD-L1 mRNA, measured by RT-PCR (technical triplicate). The relative expression of PD-L1 in the untreated cells was 1. Data, mean ± SD (n = 3). ***, P < 0.001: Fulv/Letr-treated cells versus Ctrl cells (ANOVA). H, Expression of surface PD-L1, measured by flow cytometry (technical triplicate). The dot plots are representative of one of three experiments. Percentages indicate positive cells in each quadrant. SSC: side-scatter.

Fig.4

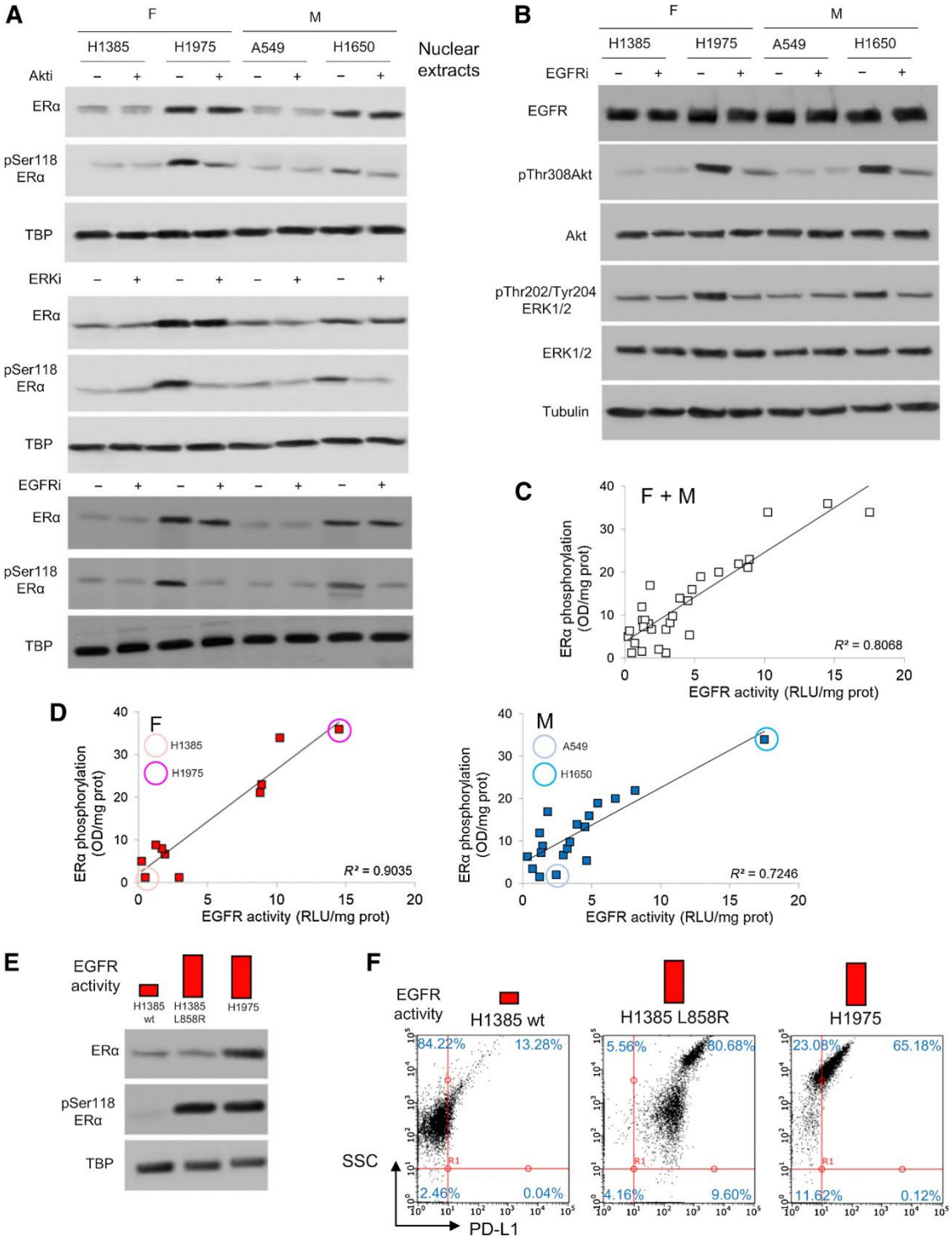

EGFR signaling controls ERα phosphorylation and PD-L1 expression. A, Female (F)-derived ERα lowNCI-H1385 and ERα highNCI-H1975 cells, male (M)-derived ERα lowA549 and ERα highNCI-H1650 cells were treated 24 h in the absence (−) or presence (+) of 1 µmol/L MK-2206, an Akt inhibitor (Akti), 10 µmol/L U-0126, an ERK-1/2 inhibitor (ERKi), 1 µmol/L AZD9291/osimertinib, an EGFR inhibitor (EGFRi), then lysed and analyzed for the indicated proteins in nuclear extracts. TBP is included as control of equal protein loading. The image is representative of one of three experiments. B, Cells were treated 24 hours in the absence (−) or presence (+) of 1 µmol/L AZD9291/osimertinib (EGFRi). The indicated proteins were measured in the whole-cell lysates. Tubulin is included as control of equal protein loading. The image is representative of one of three experiments. C, EGFR kinase activity, measured with a chemiluminescence-based assay (technical duplicates), plotted versus the amount of phospho(Ser118)ERα, measured by an ELISA assay (technical duplicates), in 29 human NSCLC cell lines. D, Data of C, disaggregated for F and M patients. E,Low EGFR

activityWild-type NCI-H1385 cells were knocked-out for endogenous EGFR and transfected with the L858R EGFR expression vector becoming EGFR-switched-on activityNCI-H1385 cells (H1385 L858R clone). NCI-H1975 cells were included as control of high EGFR activitycells. Cells were lysed and analyzed for the indicated proteins in nuclear extracts. TBP is included as control of equal protein loading. The image is representative of one of three experiments. F, Expression of surface PD-L1, measured by flow cytometry (technical triplicates), in low EGFR activitywild-type NCI-H1385 cells, EGFR-switched-on activityL858R NCI-H1385 cells, high EGFR activityNCI-H1975 cells. The dot plots are representative of one of three experiments. Percentages indicate the positive cells in each quadrant. SSC: side-scatter.

Fig.5

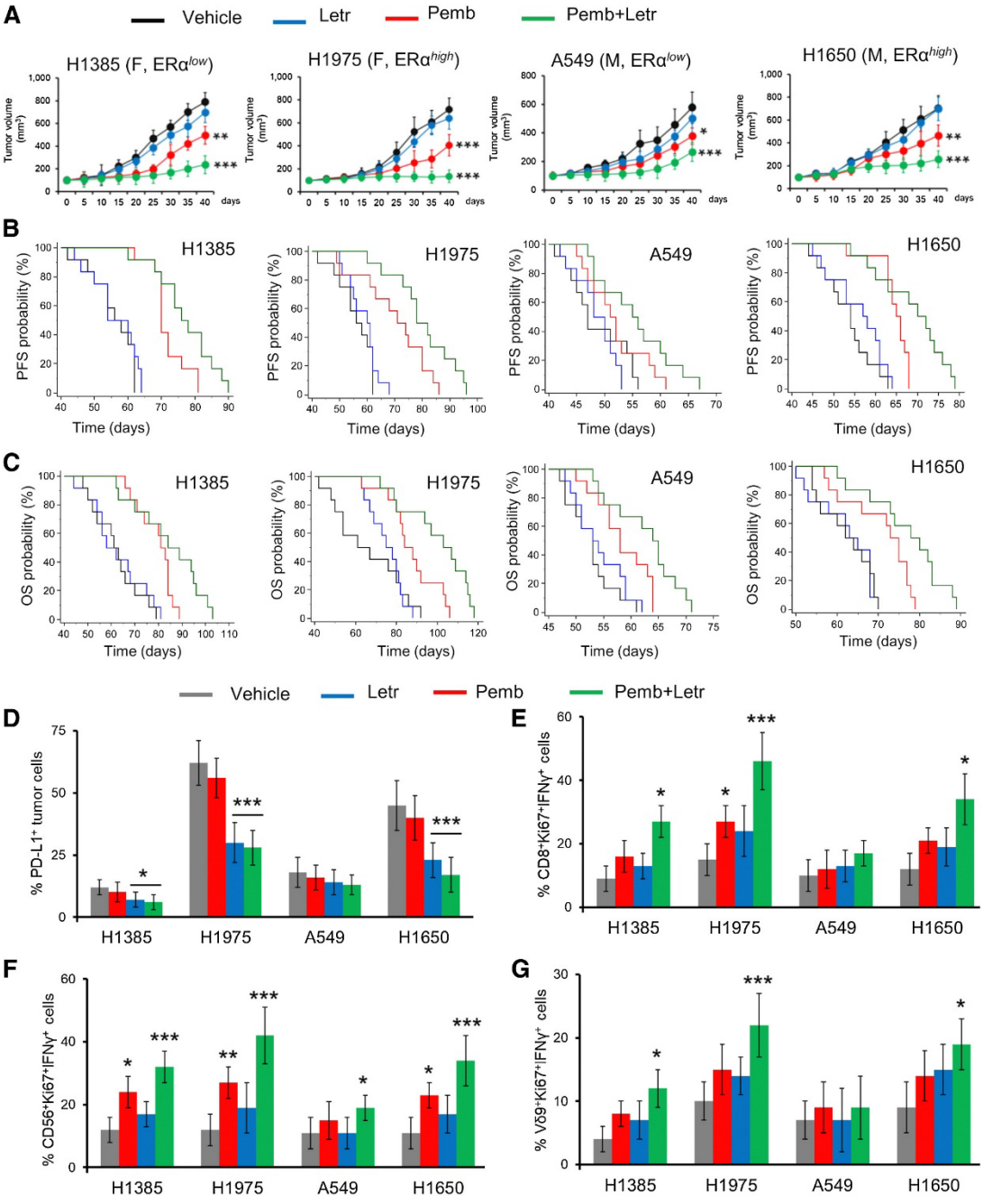

The efficacy of pembrolizumab and aromatase inhibitor is related to ERα expression in NSCLC xenografts. A, A total of 1 × 106 female-derived ERα lowNCI-H1385 cells and ERα highNCI-H1975 cells, male-derived ERα lowA549 cells and ERα highNCI-H1650 cells were implanted subcutaneously in Hu-CD34+NSG mice. When tumor reached the volume of 100 mm3, mice (n = 10/group) were randomized in the following groups: (i) Vehicle group, treated intraperitoneally with 100 µL saline solution (days 1, 7, 14, 21, 28, 35, after randomization); (ii) letrozole (Letr) group, treated with 1 mg/kg per os of 100 µL saline solution of the drug daily (days 1–35); (iii) pembrolizumab (Pemb) group, treated with 10 mg/kg i.p. of 100 µL saline solution (day 1), followed by 5 mg/kg i.p. (days 7, 14, 21, 28, and 35) of the drug; (iv) pembrolizumab + letrozole (Pemb + Letr) group, treated with 10 mg/kg i.p. of 100 µL saline solution of pembrolizumab (day 1) followed by 5 mg/kg i.p. (days 7, 14, 21, 28, and 35), and 1 mg/kg per os of 100 µL saline solution of letrozole daily (days 1–35). Tumor growth was monitored daily with a caliper. Mice were euthanized on day 40. Data, mean volumes ± SD. *, P < 0.05; **, P < 0.001; ***, P < 0.001: treatments group versus vehicle group (day 40; ANOVA). B and C, PFS and OS of tumor-bearing Hu-CD34+NSG mice, treated as reported at point A (n = 10 mice/group). P < 0.001: Pembr + Letr group versus vehicle group (PFS and OS, all groups); P < 0.001: Pembr group versus vehicle group (both PFS and OS, all groups except A549); P < 0.01: Pembr group versus vehicle group (OS, A549 group; Kaplan–Meier and log-rank test). D, PD-L1 expression was measured by

flow cytometry on dissociated tumor cells after explants (n = 10/group). *, P < 0.05; ***, P < 0.001: treatments group versus vehicle group (ANOVA). E–G, On TILs isolated from tumor extracts, the percentage of CD8+Ki67+IFNγ+cells (E), CD56+Ki67+IFNγ+cells (F), Vγ9+Ki67+IFNγ+cells (G), was measured by flow cytometry (n = 10/group). *, P < 0.05; **, P < 0.01; ***, P < 0.001: treatments group versus vehicle group (ANOVA).

Fig.6

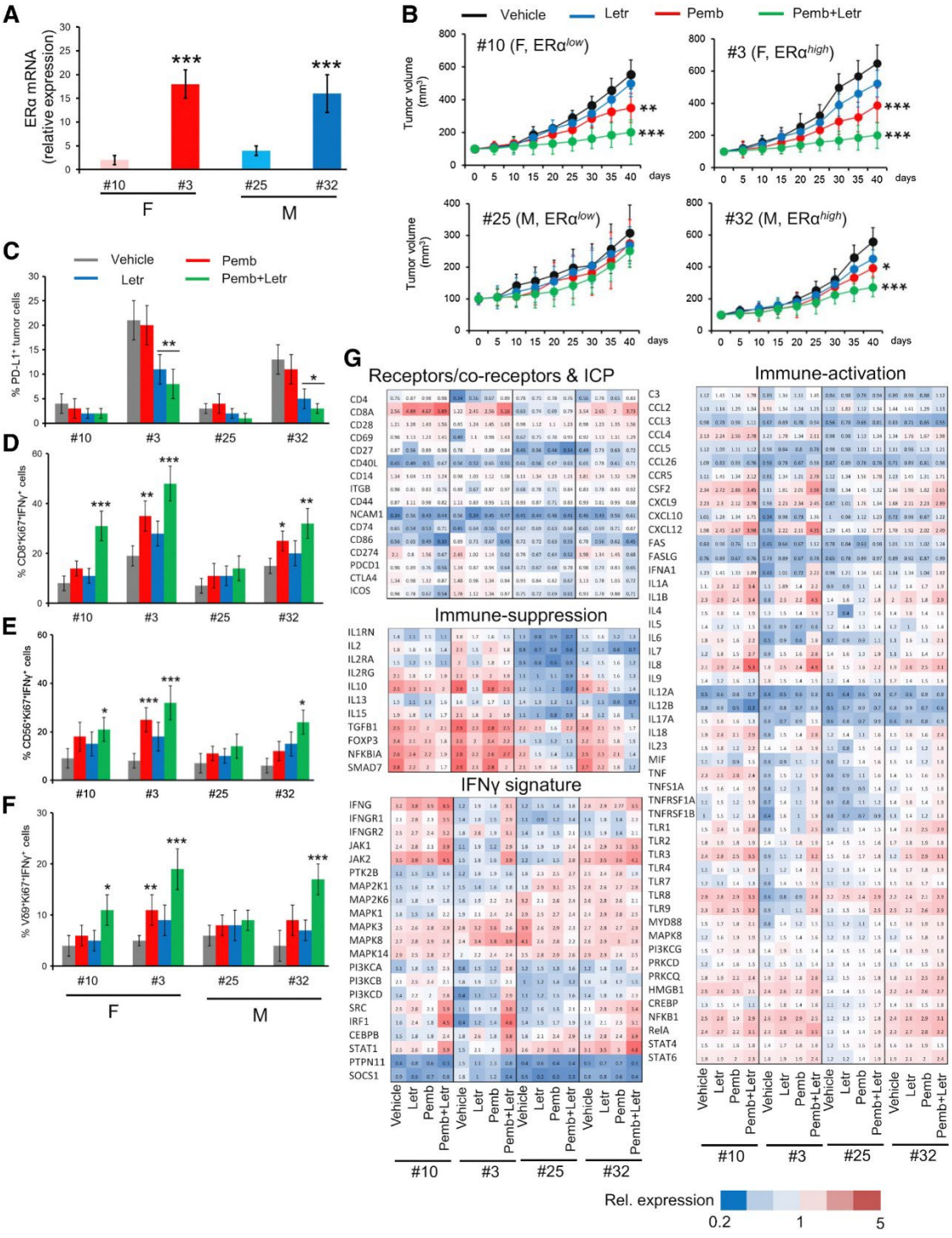

Pembrolizumab and aromatase were effective in ERαhigh immune patient-derived xenografts. A, ERα mRNA, measured by RT-PCR (technical triplicates), in cells derived from female (F) patients #10 and #3, male (M) patients #25 and #32. Data, mean ± SD (n = 3, biological replicates). ***, P < 0.001: #10 versus #3, #32 versus #25 (ANOVA). B, A total of 1 × 106 cells derived from each patient were implanted subcutaneously in Hu-CD34+NSG mice. When tumor reached the volume of 100 mm3, mice (n = 5/group) were randomized in the following groups: (i) vehicle group, treated intraperitoneally with 100 µL saline solution (days 1, 7, 14, 21, 28, 35 after randomization); (ii) letrozole (Letr) group, treated with 1 mg/kg per os of 100 µL saline solution of the drug daily (days 1–35); (iii) pembrolizumab (Pemb) group, treated with 10 mg/kg i.p. of 100 µL saline solution (day 1), followed by 5 mg/kg i.p. (days 7, 14, 21, 28, and 35) of the drug; (iv) pembrolizumab + letrozole (Pemb + Letr) group, treated with 10 mg/kg i.p. of 100 µL saline solution of pembrolizumab (day 1) followed by 5 mg/kg i.p. (days 7, 14, 21, 28, and 35), and 1 mg/kg per os of 100 µL saline solution of

letrozole daily (days 1–35). Tumor growth was monitored daily with a caliper. Mice were euthanized on day 40. Data, mean volumes ± SD. *, P < 0.05; **, P < 0.001; ***, P < 0.001: treatments group versus vehicle group (day 40; ANOVA). C, PD-L1 expression was measured by flow cytometry on dissociated tumor cells after explants (n = 5/group). *, P < 0.05; ***, P < 0.001: treatments group versus vehicle group (ANOVA). D–F, On TILs isolated from tumor extracts, the percentage of CD8+Ki67+IFNγ+cells (D), CD56+Ki67+IFNγ+cells (E), Vγ9+Ki67+IFNγ+cells (F) was measured by flow cytometry (n = 5/group). *, P < 0.05; **, P < 0.01; ***, P < 0.001: treatments group versus vehicle group (ANOVA). G, Representative heatmap of the relative expression of immune-related genes within tumor extracts, analyzed by PCR array (n = 5/group).